Theoretical Study of the 1:1 Complexes between Carbon Monoxide and Hypohalous Acids

Fernando Blanco,*,† Ibon Alkorta,† Mohammad Solimannejad,‡,§ and Jose Elguero†

Instituto de Química Médica (CSIC), Juan de la Cierva, 28006-Madrid, Spain, Quantum Chemistry Group, Department of Chemistry, Arak University, 38156-879 Arak, Iran, and Centre for Theoretical and Computational Chemistry, Department of Chemistry, University of Oslo, P.O. Box 1033, Blindern, N-0315 Oslo, Norway

Received: November 28, 2008; Revised Manuscript Received: January 30, 2009

A theoretical study of the complexes formed between carbon monoxide, CO, and the hypohalous acids (HOX, X = F, Cl, Br, and I) has been carried out using DFT [M05-2x/6-311++G(2d,2p)] and ab initio methods [(MP2/6-311++G(2d,2p) and MP2/aug-cc-pVTZ)]. Six minima were found, which correspond to two hydrogen-bonded complexes, two halogen-bonded complexes, and two van der Waals complexes. The hydrogen-bonded complexes with the carbon atom of the CO molecule are the most stable for hypohalous acids with X = F, Cl, and Br, whereas for X = I, the halogen-bonded complex with the same atom of carbon monoxide is the most stable. A blue shift in the stretching frequency of the OH bond in the hydrogen-bonded complexes with the carbon atom of CO was observed. In addition, a blue shift was observed in the bond of the hypohalous acid not involved in the interaction.

Introduction

Noncovalent interactions between molecules play a very important role in supramolecular chemistry, molecular biology, and materials science. Although research has traditionally focused on the more common hydrogen-bonded (HB) interactions, a growing body of experimental and theoretical evidence confirms the importance of other weak interactions such as the halogen bond (XB). Within this research field, hypohalous acids (HOX, where X = F, Cl, Br, and I) are a very interesting class of compounds because their structure allows them to participate in both hydrogen- (HB) and halogen- (XB) bond interactions.[1−6] The hypohalous acids are only stable in solution, with the exception of HOF, which has been isolated in the condensed state.[7] They are involved in stratospheric reactions that release free halogen molecules and atoms,[8] participating in the depletion of the ozone layer.

On the other hand, it is well-known that carbon monoxide forms complexes with transition metals. Similarly, weak gas-phase complexes of CO involving hydrogen bonds, such as those with water and its isotopic derivatives, have also been described. In both cases, the coordination occurs preferably through the C atom. Because the dipole moment of the proton acceptor, CO, is quite small [experimentally only about 0.12 D,[9] pointing from carbon (the negative end) to oxygen (the positive end)], both carbon and oxygen can interact with the proton donor to form H bonds. Along these lines, Scheiner showed theoretically that CO can participate in two different minima when it forms complexes with HF, both of which have the general structure of a H bond.[10] They are both linear, with the proton pointing toward the O or C atom: OC···HF and CO···HF. Recently, Li identified C···HN and O···HN interactions in complexes pairing CO with HNF_2, H_2NF, and HNO.[11] Vilela et al.[12] studied OH···C interactions in H_2O-CO complexes, but to our best knowledge, there has been no comprehensive comparative theoretical investigation concerning the identification of C···HO and O···HO interactions in complexes of CO with other molecular moieties.

The molecules considered in the present article, CO and hypohaloacids, are of primary importance in atmospheric chemistry.[13] Thus, we considered it appropriate to examine theoretically the different complexes that these systems can form.

Methods

The systems were optimized at the M05-2x and MP2 computational levels[14] with the 6-311++G(2d,2p) basis set[15] for all atoms, except iodine, for which the def2-TZVPP[16] basis set was used, within the Gaussian 03 package.[17] Frequency calculations were performed at the same computational level in order to confirm that the structures obtained correspond to energy minima. Additional geometry optimizations were performed at the MP2/aug-cc-pVTZ level.[18]

The use of ab initio supermolecule calculations is known to be susceptible of basis set superposition error (BSSE) when finite basis sets are used. The most common way to correct for BSSE is with the full counterpoise method.[19] Systematic studies at the restricted Hartree−Fock (RHF) level have indicated that counterpoise-corrected interaction energies are no more reliable than the uncorrected values.[20] Moreover, it has been shown[21] that uncorrected aug-cc-pVTZ binding energies lie between corrected and uncorrected aug-cc-pVQZ energies. At correlated levels, the application of the full counterpoise method causes a nonphysical increase in the dimension of the virtual space[22] that produces an overestimation of the correction.[23,24] Because the inclusion of diffuse functions has been shown to markedly reduce the BSSE effect,[25,26] the interaction energy of the clusters in the present article was calculated as the difference between the energy of the supermolecule and the sum of the energies of the isolated monomers in their minimum configuration.

The electron densities of the isolated molecules and complexes were analyzed within the atoms in molecules (AIM)

* To whom correspondence should be addressed. E-mail: fblanco@iqm.csic.es. Fax: 34-91 564 48 53.
† Instituto de Química Médica (CSIC).
‡ Arak University.
§ University of Oslo.

10.1021/jp810462h CCC: $40.75
Published on Web 03/10/2009

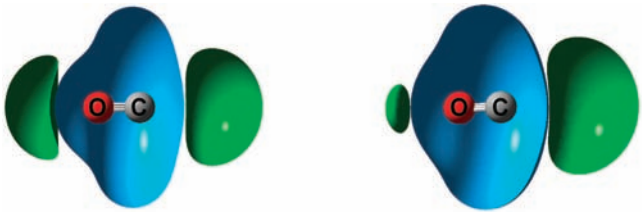

Figure 1. Representation of the MEP in the isolated CO monomer at the ±0.005 au isosurface for the (left) M05-2x/6-311++(2d,2p) and (right) MP2/6-311++(2d,2p) computational levels. Negative regions are represented in green, and positive ones are in blue.

TABLE 1: Minima of the Molecular Electrostatic Potential (au) of CO at the M05-2x/6-311++(2d,2p) and MP2/6-311++(2d,2p) Computational Levels

MEP	M05-2x/6-311++(2d,2p)	MP2/6-311++(2d,2p)
O side	−0.0104	−0.0063
C side	−0.0214	−0.0273

methodology[27] and the AIMPAC[28] and MORPHY98[29] programs. The atomic properties were obtained by integration within the atomic basins. The integration conditions were modified until the integrated Laplacian value obtained for each atom was smaller, in absolute value, than 10^{-3}, as previous studies have shown that these conditions ensure a small error in the total energy and charge of the system.[30]

The natural bond orbital (NBO) method[31] was used to analyze the interaction of the occupied and empty orbitals with the NBO-5 program.[32] This kind of interaction is of primary importance in the formation of hydrogen bonds and other charge-transfer complexes. In addition, natural energy decomposition analysis (NEDA)[33] was carried out to obtain insight into the source of the interactions. These calculations were performed within the GAMESS program.[34]

Results and Discussion

Monomers. The molecular electrostatic potential of carbon monoxide (Figure 1) shows two negative regions at the terminal positions, O side and C side (the O-side negative region is more pronounced at the M05-2x level), and one large positive region around the triple bond. The value of the molecular electrostatic potential (MEP) minimum on the carbon, clearly larger in absolute terms than that on the oxygen (Table 1), is consistent with the direction of the dipole moment, which indicates that the C side presents more negative charge than the O side.

In a previous work, we described the molecular electrostatic potential of hypohalous acids, XOH.[2] The three smaller members of this series of compounds (X = F, Cl, and Br) show two different types of minima in the MEP: one associated with the oxygen lone pair and the other with the X atom, with the minimum in the oxygen region clearly deeper than that in the X region. Thus, stronger interactions are expected between the oxygen and electron-deficient groups. The iodine derivative, hypoiodous acid, has only one minimum located on the oxygen.

Structure and Energy Analysis of the Complexes. Initially, four configurations were considered. They correspond to the possibility that the hypohalous acids can act as HB or XB donors and that the CO molecule can act as acceptor at both atoms, as indicated by the presence of negative regions in the molecular electrostatic potential at both sides of the system (Figure 1). Thus, configurations **I** and **II** are HB complexes, and configurations **III** and **IV** are XB complexes: the atoms of the carbon monoxide involved in the interaction are the oxygen for **I** and **III** and the carbon for **II** and **IV** (Scheme 1). In addition, we

SCHEME 1: Structures of the Complexes between HOX and CO Studied in This Work

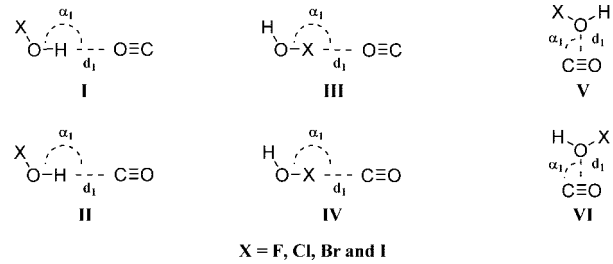

considered the possibility of two van der Waals (vdW) complexes (**V** and **VI**) between the lone pairs of the oxygen atom of the hypohalous derivatives and the molecular electrostatic positive region that surrounds the triple bond of carbon monoxide. Even though, in general, π systems do not act as electron acceptors, some cases have been described in the literature where the effect of electron-withdrawing moieties favor their interactions with electron donors.[35]

We located the minima of the six structures (five at the MP2 level) for all of the acids studied except the fluorine derivatives (Figure 2). For these derivatives, only three minima were obtained, two corresponding to the HB complexes (**I** and **II**) and another one corresponding to a special type of XB complex with the F atom oriented toward the bonding region of the carbon monoxide in an intermediate disposition between the C and O atoms. The vdW complexes are not stable structures for hypofluorous acid because they revert to the previously found minima.

The energy results (Table 2) show that, for any given case, the interaction values, although not identical, follow the same trend for the three calculation methods. Thus, linear correlations are found between the three methods, with square correlation coefficients of 0.93 and 0.88 for M05-2x/6-311++(2d,2p) results compared to the MP2/6-311++(2d,2p) and MP2/aug-cc-pvtz results, respectively. These correlations increase significantly (0.95 and 0.93, respectively) if the weakest interactions, **V** and **VI**, are not considered. In general, the DFT functional M05-2x slightly underestimates the relative energy values with respect to those obtained at the MP2 level with the same basis set. Exceptions are the energy values obtained for the complexes in configuration **I** of FOH:CO and ClOH:CO, where the interaction energies calculated at the M05-2x level are larger than those calculated at the MP2 level, probably because of the differences observed in the geometry of the complexes that will be discussed latter. Thus, this inexpensive method provides similar qualitative results to the more expensive MP2 approach.

An analysis of the interaction energies obtained within each configuration shows similar values for the HB and vdW complexes (**I**, **II**, **V**, and **VI**), independently of the hypohalous acid considered. In contrast, the nature of the halogen atoms has a strong influence on the values obtained for the XB complexes (**III** and **IV**).

More significant are the differences related to the type of coordination, HB, XB, or vdW. In general, the vdW complexes are the least stable minima, and thus, at the MP2 level, one of them reverts to another more stable minimum. On the other hand, within the HB and XB systems, there are considerable energy differences depending on the interaction site of the CO donor species, O side or C side, with the latter always being more stable. These results can be rationalized on the basis of the molecular electrostatic potential for the isolated CO molecule

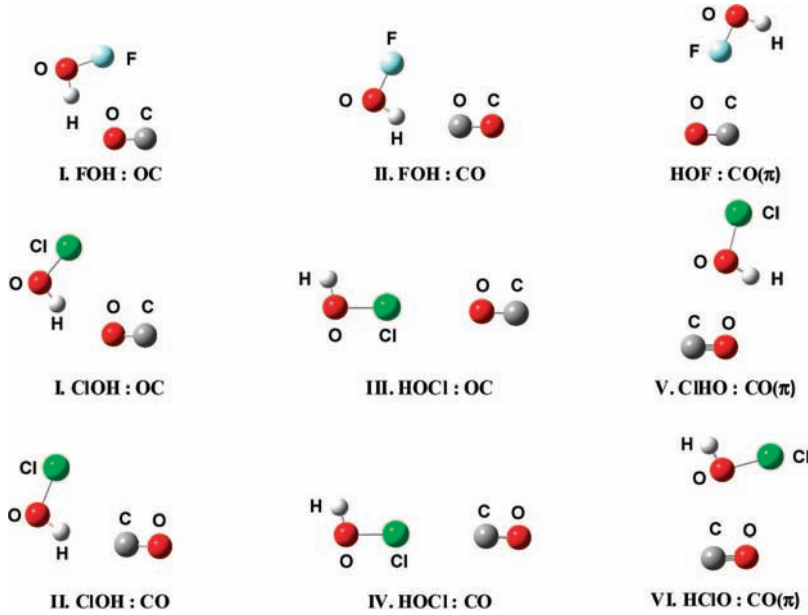

Figure 2. Some examples of the minimum-energy complexes between HOX and CO located in this work at the M05-2x/6-311++(2d,2p) computational level.

TABLE 2: Interaction Energies (kJ mol^{-1})

complex	configuration	M05-2x/6-311+ +G(2d, 2p)	MP2/6-311+ +G(2d, 2p)	MP2/aug-cc-pVTZ
FOH:OC	**I**	−7.84	−6.70	−6.85
ClOH:OC	**I**	−7.91	−7.30	−7.78
BrOH:OC	**I**	−7.42	−7.19	−8.34
IOH:OC	**I**	−7.27	−7.49	
FOH:CO	**II**	−12.33	−15.20	−15.99
ClOH:CO	**II**	−12.89	−15.81	−17.05
BrOH:CO	**II**	−12.33	−15.32	−17.55
IOH:CO	**II**	−11.58	−15.54	
HOCl:OC	**III**	−4.26	−5.02	−4.74
HOBr:OC	**III**	−4.84	−5.65	−7.08
HOI:OC	**III**	−6.65	−7.67	
HOCl:CO	**IV**	−6.38	−7.51	−7.98
HOBr:CO	**IV**	−8.79	−10.92	−14.03
HOI:CO	**IV**	−14.23	−17.62	
HOCl:CO(π)	**V**	−5.56	*a*	*a*
HOBr:CO(π)	**V**	−4.15	*a*	*a*
HOI:CO(π)	**V**	−5.09	*a*	
HOCl:CO(π)	**VI**	−5.02	−4.96	−4.96
HOBr:CO(π)	**VI**	−5.11	−5.35	−6.06
HOI:CO(π)	**VI**	−6.20	−6.10	

[a] These structures spontaneously revert to another minimum.

TABLE 3: Interacting Distances and Angles Calculated at the MP2/6-311++(2d,2p) and M05-2x/6-311++(2d,2p) Computational Levels[a]

		MP2/6-311+ +(2d,2p)		M05-2x/6-311+ +(2d,2p)	
complex	configuration	d_1	α_1	d_1	α_1
FOH:OC	**I**	2.203	174.5	2.227	135.2
ClOH:OC	**I**	2.197	175.0	2.221	151.9
BrOH:OC	**I**	2.206	176.8	2.232	160.0
IOH:OC	**I**	2.207	176.8	2.239	174.2
FOH:CO	**II**	2.166	175.9	2.242	171.0
ClOH:CO	**II**	2.152	177.1	2.243	172.2
BrOH:CO	**II**	2.164	177.7	2.249	173.3
IOH:CO	**II**	2.165	178.0	2.264	179.0
HOCl:OC	**III**	3.081	179.9	3.102	179.4
HOBr:OC	**III**	3.125	179.9	3.126	179.9
HOI:OC	**III**	3.170	179.9	3.165	179.9
HOCl:CO	**IV**	3.059	179.7	3.088	179.3
HOBr:CO	**IV**	2.978	179.8	3.006	179.8
HOI:CO	**IV**	2.921	179.8	2.962	179.7
HOCl:CO(π)	**V**	−	−	2.995	103.2
HOBr:CO(π)	**V**	−	−	3.081	90.4
HOI:CO(π)	**V**	−	−	3.170	89.5
HOCl:CO(π)	**VI**	3.138	87.9	3.087	84.6
HOBr:CO(π)	**VI**	3.115	88.8	3.070	86.3
HOI:CO(π)	**VI**	3.083	88.9	3.048	84.6

[a] Parameters defined in Scheme 1.

(Figure 1), where a deeper electrostatic minimum is obtained on the carbon side. A number of experimental studies of gas-phase complexes have confirmed the preference for the C side in interactions with electron-poor atoms.[36−39]

The most stable configuration for the smallest hypohalous acids (X = F, Cl, Br) corresponds to the HB complex. Hypoiodous acid, in contrast, shows the highest stability for the halogen-bonded complex. These findings are in agreement with previous theoretical results for the complexes of hypohalous acids with nitrogenated basis[2] and with experimental detection using microwave spectroscopy of the HB (IH···CO) and XB (HI···CO) complexes between hydrogen iodide and carbon monoxide.[40,41]

A selection of the geometrical parameters of the optimized complexes has been gathered in Table 3. Even though significant correlations were not established because of the variety of interactions, the values obtained at M05-2x and MP2 the levels present similar trends. In general, the shortest distances correspond to the HB complexes and always those involving the C side. The chlorine **II** derivative shows the smallest distance (d_1) among the MP2 results, corresponding to the second most stable structure, and the iodine **IV** derivative has a very short interaction distance, considering the radius of iodine and the distances of the other XB systems, in agreement with the high stability found for this complex. In relation to the α_1 angle, is interesting to note that, at the MP2 level, each of the complexes **I**−**IV** shows an essentially linear disposition of the interacting

TABLE 4: Bond Stretching Frequencies of the Monomers (in Italics) and Variation upon Complexation (cm^{-1}) Calculated at the MP2/6-311++G(2d,2p) Computational Level

system	configuration	OH stretching	OX stretching	CO stretching
CO				*2113.5*
HOF		*3797.2*	*954.8*	
HOCl		*3803.5*	*729.7*	
HOBr		*3799.7*	*628.2*	
HOI		*3805.4*	*588.7*	
FOH:OC	**I**	5.8	2.8	−1.9
FOH:CO	**II**	−77.5	1.2	20.7
HOF:CO(π)	**III**	−2.6	−2.1	0.0
ClOH:OC	**I**	3.7	3.2	−2.9
ClOH:CO	**II**	−88.3	4.0	18.7
HOCl:OC	**III**	4.7	−2.6	−2.3
HOCl:CO	**IV**	7.8	−8.3	6.2
HOCl:CO(π)	**VI**	−4.0	−1.5	0.2
BrOH:OC	**I**	5.1	3.2	−3.1
BrOH:CO	**II**	−83.3	5.5	18.9
HOBr:OC	**III**	1.7	−3.1	−3.3
HOBr:CO	**IV**	7.0	−12.5	10.1
HOBr:CO(π)	**VI**	−4.3	−1.6	0.9
IOH:OC	**I**	1.1	2.9	−3.5
IOH:CO	**II**	−86.8	6.1	18.4
HOI:OC	**III**	1.6	−1.7	−4.4
HOI:CO	**IV**	8.8	−11.3	11.6
HOI:CO(π)	**VI**	−7.2	−0.4	−1.7

HOX atom with respect to CO (close to 180°). The trend is similar at the M05-2x level, except for complex type **I**, for which this angle decreases as the size of the halogen decreases.

For complexes **V** and **VI**, d_1 is the distance between the HOX oxygen and the central point of the CO bond, and α_1 is the C_{CO}—center$_{CO}$—O_{HOX} angle, which provides an idea of the deviation with respect to the perpendicular of HOX compared to the CO unit. Once again, the expected trend is confirmed, as the most strongly stabilized complexes [HOCl:CO(π) (**V**) and HOI:CO(π) (**VI**)] show the shortest distances of interaction. Regarding α_1, the values at the M05-2x level show that, for type **VI** complexes, the HOX oxygen is located close to the perpendicular line but always deviated toward the carbon side of CO ($\alpha_1 < 90°$), whereas for the **V** complexes, there is a trend to approach the terminal oxygen ($\alpha_1 > 90°$) for the smaller halogen derivatives (chlorine and bromine).

Stretching Frequencies. Hydrogen-bond formation has been associated to a red shift in the stretching frequency of the HB donor.[42] However, recently, an increasing number of cases have been described in the literature for which complex formation is associated with blue shifts.[43] The bond stretching frequencies, calculated in the present article, are listed in Table 4. A small blue shift, between 1 and 6 cm^{-1}, is observed in the OH frequency for all of the complexes in configuration **I** where the interaction is with the oxygen of carbon monoxide. In contrast, large red shifts, between 77 and 88 cm^{-1}, are observed for the same stretching frequency when the HB acceptor atom is the carbon (configuration **II**). In the case of XB interactions, a red shift of the XB stretching frequency is observed in both configurations **III** and **IV**, being larger in the latter case. For the complexes in configuration **VI**, a red shift is observed for both OH and OX bonds. Interestingly, the bond of the hypohalous acid not involved in the interaction suffers a blue shift in both HB and XB complexes (configurations **I**—**IV**). A similar feature has been described for the complexes between hypohalous acids and nitrosyl hydride.[4]

Finally, the bond stretching of carbon monoxide shows small red shifts when the HB and XB interactions are with the oxygen atom, whereas larger blue shifts are observed when the interacting atom is the carbon. In the case of the π complexes, the variations are smaller and can be positive or negative.

A parabolic relationship was found between the CO bond stretching and the bond length as shown in Figure 3. Similarly, in the other cases (OH and OX bonds), interesting trends were found, but without enough points to establish consistent correlations.

Natural Bond Orbital Analysis. An NBO analysis was performed to evaluate several different electronic properties of the systems. Table 5 lists the most significant parameters of the NBO study. Initially, the analysis of the NBO charges gives a first approximation of the type of coordination that has been established in the complexes. A small charge transfer is observed between the interacting molecules in the minimum complexes between carbon monoxide and the hypohalous acids, except for the complexes in configuration **IV**, where the opposite occurs. The amount of this transfer is dependent on the strength of the interaction; thus, the largest transfer is observed for the C-side complexes, **II** and **IV**, for both HB and XB interactions, whereas for the O-side, coordinated, and vdW systems, charge transfer does not occur or is very small. Moreover, for the C-side structures, it can be observed that the charge transfer is highly dependent on the halogen atom in the type **IV** complexes formed by halogen bonds, whereas it is very similar for all of the type **II** complexes formed by hydrogen bonds, where the effects of the electronegativity and size of the halogen do not significantly affect the interacting H atom.

Table 5 reports the stabilization energy values of the orbital interaction within the NBO analysis. In complexes **I**—**IV**, this interaction occurs from the lone pair of the CO interacting atom (donor species) to the antibonding orbital of the involved HOX bond (acceptor species), namely, H—O in the HB systems and X—O in the XB systems. In the vdW complexes (**V** and **VI**), the roles of the monomers reverse, and CO becomes the acceptor species while HOX becomes the donor species. In this case, the orbital interaction occurs between the lone pair of the HOX oxygen atom and the antibonding orbital of the CO system.

As expected, for both HB and XB complexes, we found significant stabilizing orbital interactions that are more effective in the case of complexes **II** and **IV**. This result is consistent with the above-discussed analysis of charge transfer. The nature of the halogen atom slightly affects the **I** and **II** HB complexes. Thus, as the electronegativity of the halogen increases, from iodine to fluorine, a small increment in the value of the orbital interaction is observed, probably because of the enhancement of the acceptor capacity of the interacting hydrogen as a result of the inductive effect of the halogen. In the XB complexes (**III** and **IV**), the dependence of the value of the orbital interaction on the halogen is more pronounced, especially in the case of type **IV** complexes. As its size increases, the halogen atom becomes less electronegative and more polarizable, and thus, it becomes more positively charged, which favors its interaction with electron donors. The specific case of the iodine complex in configuration **IV** (HOI:CO) has, by far, the largest value of the orbital interaction, which could explain the high stability of this complex. On the other hand, the values of the orbital interaction in the vdW complexes, **V** and **VI**, are very small, which is consistent with the results of the charge-transfer analysis described before.

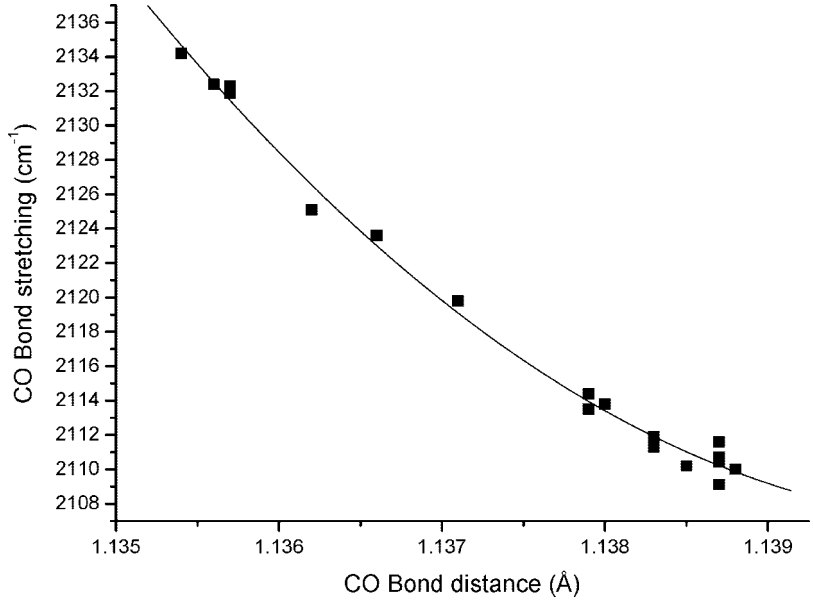

Figure 3. Bond stretching vs bond distance for the CO molecule calculated at the MP2/6-311++G(2d,2p) computational level. The parabolic fitting presents a square correlation coefficient of 0.992.

TABLE 5: NBO Analysis and NEDA at the M05-2x/6-311++(2d,2p) Computational Level

				natural energy decomposition analysis (NEDA) (kJ mol^{-1})					
complex	configuration	charge transfer (e)	orbital interaction (kJ mol^{-1})	CT	ES	POL	XC	DEF (CO)	DEF (HOX)
FOH:OC	**I**	0.000	3.01	−15.48	−7.15	−14.02	−10.00	12.59	27.53
ClOH:OC	**I**	0.000	3.51	−15.61	−6.86	−14.06	−9.33	14.39	24.94
BrOH:OC	**I**	0.000	3.22	−15.15	−6.74	−14.69	−9.20	15.56	23.85
IOH:OC	**I**	0.000	3.01	−14.23	−5.90	−12.18	−7.70	15.23	19.29
FOH:CO	**II**	0.014	27.24	−40.92	−16.78	−2.22	−8.45	34.64	22.22
ClOH:CO	**II**	0.013	26.69	−42.09	−17.11	−6.07	−10.13	40.79	22.76
BrOH:CO	**II**	0.012	24.81	−40.29	−16.95	−8.03	−10.59	42.13	22.09
IOH:CO	**II**	0.012	22.13	−34.77	−14.60	−2.01	−8.58	33.76	15.98
HOCl:OC	**III**	0.001	1.88	−9.92	−2.85	−15.65	−7.41	13.68	19.04
HOBr:OC	**III**	0.002	3.72	−12.22	−4.10	−24.89	−9.71	21.97	25.06
HOI:OC	**III**	0.002	6.28	−15.69	−6.11	−23.89	−12.34	18.87	33.56
HOCl:CO	**IV**	0.010	9.75	−21.67	−9.25	−34.73	−12.26	52.43	20.38
HOBr:CO	**IV**	0.022	24.56	−42.09	−17.15	−77.99	−18.07	114.10	33.14
HOI:CO	**IV**	0.034	49.29	−75.60	−28.24	−48.99	−29.04	114.60	53.51
HOCl:CO(π)	**V**	0.002	0.21	−9.62	−5.15	−15.98	−10.13	16.78	19.83
HOBr:CO(π)	**V**	0.001	0.59	−7.74	−4.23	−11.84	−7.70	14.31	13.77
HOI:CO(π)	**V**	0.001	0.54	−8.12	−5.02	−14.98	−9.04	17.61	15.73
HOCl:CO(π)	**VI**	−0.001	2.13	−9.33	−4.06	−13.26	−9.67	13.35	19.25
HOBr:CO(π)	**VI**	−0.001	0.92	−10.29	−4.52	−17.03	−11.13	17.11	21.71
HOI:CO(π)	**VI**	−0.001	0.84	−12.22	−5.48	−20.04	−12.76	21.09	24.60

Natural energy decomposition analysis (NEDA) is a method for partitioning molecular interaction energies including charge transfer (CT), electrostatic (ES), polarization (POL), and core repulsion (DEF) contributions. The charge-transfer term is based on the interaction of filled orbitals (donors) with empty ones (acceptors) for the species involved. Taking into account the fact that, in the studied systems, because both the donor and the acceptor molecules have different positions available to coordinate, the best stabilization occurs when the atom with the highest electron density of the donor species interacts with the atom with greatest capacity to accommodate the charge in the acceptor species. In the CO molecule, the negative electron density is located on the carbon. As can be seen in Table 5, the contribution of the CT component is most significant in the complexes where C is the coordinating site (**II** and **IV**), keeping, in all cases, the same halogen dependency as observed in the NBO charge-transfer and orbital analyses. On the other hand, the electrostatic component of the interaction is mostly related to a more favorable orientation of the coordinating species according to its local dipole moment. The systems studied in this work are very small, and it is easy to identify the dipole on the basis of the distribution of electron density. The trends observed in all cases are very similar to the analysis based on the donor−acceptor character: the electrostatic component is again higher in complexes **II** and **IV**, but in relative terms, the overall weight of the ES contribution is greater in complexes **I** and **III**, because they have reduced CT components. The polarization component (POL) becomes the

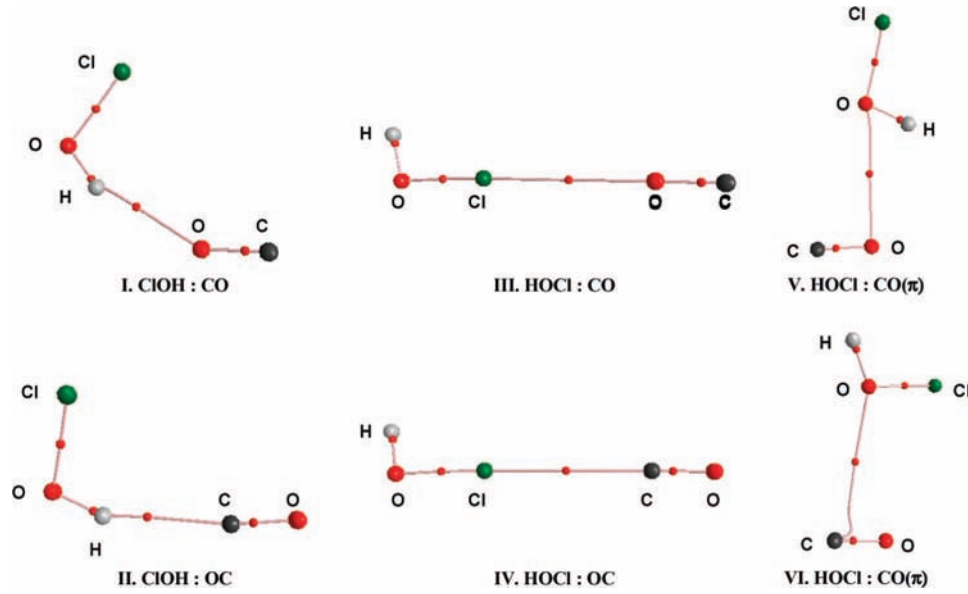

Figure 4. Molecular graph of the chlorine derivatives at the M05-2x/6-311++(2d,2p) computational level. Red balls indicate the bond critical points.

most important stabilizing term in the XB complexes (**III** and **IV**), increasing its absolute value for a given configuration as the size of the halogen atom increases. For complexes **V** and **VI**, we can note a higher influence of charge-transfer and polarization components of the interaction with respect to the electrostatic component.

Repulsion between the cores is another of the basic components in the NEDA and is measured according to the deformation of the electronic clouds (DEF). This kind of interaction is opposed to the bond and is, in general, more pronounced in the case of structures with stronger interactions, in which the nuclei are closer. In our case, the NEDA distinguishes two separate subunits (CO and HOX) involved in the complexes. As shown in Table 5, the variation of the deformation values is most pronounced on the CO side of the complexes and within them in the systems that exhibited better stability in the energy analysis. The deformation values for the vdW complexes are smaller than those found for the rest of the complexes.

Electron Density Analysis. The topological analysis of the electron density shows the presence of an intermolecular bond critical point (BCP) in all of the complexes, HB, XB, and vdW (Figure 4). In all cases, these BCPs show small values of the electron density and positive Laplacians, an indication of the closed-shell characteristics of the interaction (Table 6), similar to those found in weak interactions.[44,45]

The electron densities at the BCPs and the bond distances in the HB and XB complexes present an exponential relationship similar to that described for other HB complexes,[46,47] but there are not enough points for each kind of complex to obtain a significant correlation.

Interestingly, an oxygen−oxygen BCP was found in configuration **V**. Similar BCPs have been reported in previous works, and they were associated with an extra stabilization of those configurations compared to others that do not present the mentioned BCP.[48,49] Another interesting feature of the molecular graph of this system is the dependency of the intermolecular bond path on the angle between the interacting oxygen and the CO molecule. In the case of ClOH:CO (configurations **V** and **VI**), the BCP obtained is with the oxygen when the O···CO angle is smaller than 84° but with the carbon atom when the angle is larger. This result is indicative of the presence of a catastrophic point in the description of the electron density around this angle value.[27,50]

TABLE 6: Electron density (au) calculated at the M05-2x/6-311++(2d,2p) computational level

complex	configuration	ρ	Laplacian
FOH:OC	**I**	0.0109	0.0452
ClOH:OC	**I**	0.0107	0.0449
BrOH:OC	**I**	0.0103	0.0437
IOH:OC	**I**	0.0100	0.0427
FOH:CO	**II**	0.0157	0.0487
ClOH:CO	**II**	0.0157	0.0488
BrOH:CO	**II**	0.0155	0.0482
IOH:CO	**II**	0.0147	0.0461
HOCl:OC	**III**	0.0060	0.0280
HOBr:OC	**III**	0.0071	0.0314
HOI:OC	**III**	0.0084	0.0344
HOCl:CO	**IV**	0.0095	0.0368
HOBr:CO	**IV**	0.0139	0.0491
HOI:CO	**IV**	0.0187	0.0599
HOCl:CO(π)	**V**	0.0078	0.0325
HOBr:CO(π)	**V**	0.0062	0.0231
HOI:CO(π)	**V**	0.0065	0.0242
HOCl:CO(π)	**VI**	0.0063	0.0241
HOBr:CO(π)	**VI**	0.0065	0.0250
HOI:CO(π)	**VI**	0.0070	0.0264

A linear relationship was found between the electron density at the intermolecular bond critical point and the corresponding interaction energy of the complexes (Figure 5). The values of the square correlation coefficients are 0.99, 0.96, and 0.44 for HB, XB, and vdW interactions, respectively, and 0.96 for the overall series. Similar linear relationships have been described before for some hydrogen-bonded systems.[51]

The integration of the properties within the atomic basins provides a tool for analyzing the variation of the energy, charge, and volume associated with complex formation (Table 7). An energy stabilization of the hypohalous acid is observed upon complexation. This stabilization is increased from HOF to HOBr and compensates, in all cases, for the destabilization that takes

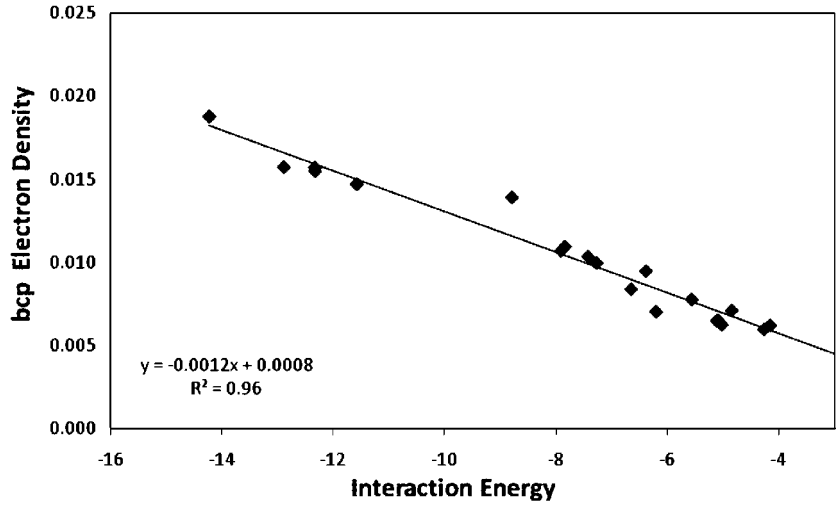

Figure 5. Interaction energy vs electron density of the intermolecular BCP in all of the complexes calculated at the M05-2x/6-311++(2d,2p) computational level.

TABLE 7: Variations in the Properties of the Hypohalous Acids and CO upon Complexation and Total Complex Volume Obtained Using the AIM Methodology at the M05-2x/6-311++(2d,2p) Computational Level

complex	configuration	ΔE(HOX) (kJ mol^{-1})	charge(HOX) (e)	ΔV(HOX) (au)	ΔE(CO) (kJ mol^{-1})	ΔV(CO) (au)
FOH:OC	**I**	−44.93	−0.006	−3.52	37.06	−7.10
FOH:CO	**II**	−57.84	−0.025	−1.40	45.80	−11.69
HOF:CO(π)		−43.34	−0.005	0.79	40.29	−1.87
ClOH:OC	**I**	−79.10	−0.001	−2.86	71.69	−4.33
ClOH:CO	**II**	−94.36	−0.019	−2.91	82.36	−10.52
HOCl:OC	**III**	−80.87	0.003	0.06	76.88	−1.36
HOCl:CO	**IV**	−83.46	−0.011	−0.55	77.34	−3.62
HClO:CO(π)	**V**	−75.76	−0.003	−1.81	70.37	−4.53
HClO:CO(π)	**VI**	−70.81	−0.004	−1.13	72.03	−0.17
BrOH:OC	**I**	−406.48	0.000	−2.95	399.28	−4.03
BrOH:CO	**II**	−421.33	−0.018	−3.11	409.82	−10.08
HOBr:OC	**III**	−406.99	0.003	−2.07	402.43	−2.15
HOBr:CO	**IV**	−417.07	−0.017	−3.50	408.62	−8.32
BrHO:CO(π)	**V**	−400.93	−0.002	−0.89	398.02	−1.64
HBrO:CO(π)	**VI**	−400.47	0.000	−2.33	396.66	−0.36

place in the CO molecule as a result of coordination, probably through the deformation of the electronic structure and loss of charge by transfer. In general, a charge transfer is observed from CO to the hypohalous acids following the same trends as those described in the NBO analysis and confirming structure types **II** and **IV** as the clearest complexes of the "charge-transfer" type in the series.

Analysis of the volume variations shows, with only one exception [HOCl:OC (**III**)], that the coordination produces a contraction of the two parts of the complex. This contraction is, in general, most pronounced in systems with strong stabilization, coinciding with the reduction of the interaction distance described in relation to the structural analysis.

Conclusion

A theoretical study of the 1:1 complexes formed by carbon monoxide and the hypohalous acids (HOX, X = F, Cl, Br, and I) has been carried out by means of DFT and ab initio methods. Up to six minimum configurations were found: two HB, two XB, and two vdW complexes. In the vdW complexes, the interaction occurs between the oxygen of the hypohalous acid and the π cloud of carbon monoxide.

The complexes with the carbon-atom end of carbon monoxide are more stable than those with the oxygen-atom end. In the same way, the smallest hypohalous acids (X = F, Cl, and Br) prefer the formation of HB complexes, XOH···CO, whereas for iodine, the XB complex, HOI···CO, is the absolute minimum. The vibrational analysis of the studied complexes showed a significant red shift of the OH bond, about 80−90 cm $^{-1}$, in complexes with OH···C interactions, whereas small blue shifts were found when the HB interaction was with the oxygen atom of carbon monoxide. In addition, a blue shift in the stretching frequencies in the bond in the hypohalous acid not involved in the interaction was found for both HB and XB complexes.

NBO analysis and NEDA indicate the importance of the intermolecular orbital interaction in the stabilization of the complexes. Thus, the charge-transfer term is most important in the HB complexes and in the most stable XB complexes. Only in the XB complexes with Cl and Br is the polarization term the most important attractive term.

Finally, a linear correlation was found between the electron density at the intermolecular BCP and the strength of the interaction.

Acknowledgment. The authors acknowledge financial support from the Spanish Ministerio de Educación y Ciencia (Project CTQ2007-61901/BQU) and the Comunidad Autónoma

de Madrid (Project MADRISOLAR, ref S-0505/PPQ/0225). M.S. acknowledges a travel grant provided by the Centre for Theoretical and Computational Chemistry (CTCC) at the University of Oslo. Thanks are given to CTI (CSIC) for allocation of computer time.

Supporting Information Available: Cartesian coordinates of the optimized complexes at the MP2/6-311++G(2d,2p) computational level. This information is available free of charge via the Internet at http://pubs.acs.org.

References and Notes

(1) Solimannejad, M.; Alkorta, I.; Elguero, J. *Chem. Phys. Lett.* **2008**, *454*, 201.
(2) Alkorta, I.; Blanco, F.; Solimannejad, M.; Elguero, J. *J. Phys. Chem. A* **2008**, *112*, 10856.
(3) Politzer, P.; Murray, J. S.; Concha, M. C *J. Mol. Model.* **2008**, *14*, 659.
(4) Solimannejad, M.; Scheiner, S. *J. Phys. Chem. A* **2008**, *112*, 4120.
(5) Solimannejad, M.; Alkorta, I.; Elguero, J. *Chem. Phys. Lett.* **2007**, *449*, 23.
(6) Solimannejad, M. Pejov, Lj. *J. Phys. Chem. A* **2005**, *109*, 825.
(7) Poll, W.; Pawelke, G.; Mootz, D.; Appelman, E. H. *Angew. Chem., Int. Ed. Engl.* **1988**, *27*, 392.
(8) (a) Molina, M. J.; Tso, T. L.; Molina, L. T.; Wang, F. C. *Science* **1987**, *238*, 1253. (b) Tolbert, M. A.; Rossi, M. J.; Malhotra, R.; Golden, D. M. *Science* **1987**, *238*, 1258.
(9) Gu, Q. Y.; Lou, S. C. *Table of Chemical Materials*; Jiangsu Science and Technology Press: Jiangsu, China, 1998.
(10) Scheiner, S. *Hydrogen Bonding*; Oxford University Press: New York, 1997.
(11) Li, A. Y. *J. Phys. Chem. A* **2006**, *110*, 10805.
(12) Vilela, A. F. A.; Barreto, P. R. P.; Gargano, R.; Cunha, C. R. M. *Chem. Phys. Lett.* **2006**, *427*, 29.
(13) (a) Rowland, F. S.; Molina, M. J. *Rev. Geophys.* **1975**, *13*, 21. (b) Rycroft, M. J. *Geogr. J.* **1990**, *156*, 1. (c) McGrath, M. P.; Rowland, F. S. *J. Phys. Chem.* **1996**, *100*, 4815.
(14) Møller, C.; Plesset, M. S. *Phys. Rev.* **1934**, *46*, 618.
(15) Frisch, M. J.; Pople, J. A.; Binkley, J. S. *J. Chem. Phys.* **1984**, *80*, 3265.
(16) Weigend, F.; Ahlrichs, R. *Phys. Chem. Chem. Phys.* **2005**, *7*, 3297.
(17) Frisch, M. J.; Trucks, G. W.; Schlegel, H. B.; Scuseria, G. E.; Robb, M. A.; Cheeseman, J. R.; Montgomery, J. A., Jr.; Vreven, T.; Kudin, K. N.; Burant, J. C.; Millam, J. M.; Iyengar, S. S.; Tomasi, J.; Barone, V.; Mennucci, B.; Cossi, M.; Scalmani, G.; Rega, N.; Petersson, G. A.; Nakatsuji, H.; Hada, M.; Ehara, M.; Toyota, K.; Fukuda, R.; Hasegawa, J.; Ishida, M.;. Nakajima, T.; Honda, Y.; Kitao, O.; Nakai, H.; Klene, M.; Li, X.; Knox, J. E.; Hratchian, H. P.; Cross, J. B.; Bakken, V.; Adamo, C.; Jaramillo, J.; Gomperts, R.; Stratmann, R. E.;. Yazyev, O.; Austin, A. J.; Cammi, R.; Pomelli, C.; Ochterski, J. W.; Ayala, P. Y.;. Morokuma, K.; Voth, G. A.; Salvador, P.; Dannenberg, J. J.; Zakrzewski, V. G.; Dapprich,. S.; Daniels, A. D.; Strain, M. C.; Farkas, O.; Malick, D. K.; Rabuck, A. D.; Raghavachari,. K.; Foresman, J. B.; Ortiz, J. V.; Cui, Q.; Baboul, A. G.; Clifford, S.; Cioslowski, J.;. Stefanov, B. B.; Liu, G.; Liashenko, A.; Piskorz, P.; Komaromi, I.; Martin, R. L.; Fox, D. J.;. Keith, T.; Al-Laham, M. A.; Peng, C. Y.; Nanayakkara, A.; Challacombe, M.; Gill, P. M. W.; Johnson, B.; Chen, W.; Wong, M. W.; Gonzalez, C.; Pople, J. A. *Gaussian 03*; Revision E.01, Gaussian, Inc.: Wallingford, CT, 2003.
(18) Dunning, T. H. *J. Chem. Phys.* **1989**, *90*, 1007.
(19) Boys, S. F.; Bernardi, F. *Mol. Phys.* **1970**, *19*, 553.
(20) Schwenke, D. W.; Truhlar, D. G. *J. Chem. Phys.* **1985**, *82*, 2418.
(21) Del Bene, J. E.; Shavitt I. In *Molecular Interactions: From Van der Waals to Strongly Bound Complexes*; Scheiner, S. J., Ed.; Wiley: Sussex, U.K., 1997; pp 157−179.
(22) Cook, D.B.; Sordo, J. A.; Sordo, T. L. *Int. J. Quantum Chem.* **1993**, *48*, 375.
(23) Frey, J. A.; Leutwyler, S. *J. Phys. Chem. A* **2005**, *9*, 6990.
(24) Frey, J. A.; Leutwyler, S. *J. Phys. Chem. A* **2006**, *10*, 12512.
(25) Frisch, M. J.; Del Bene, J. E.; Binkley, J. S.; Schaefer, H. F., III *J. Chem. Phys.* **1986**, *84*, 2279.
(26) King, B. F.; Weinhold, F. *J. Chem. Phys.* **1995**, *103*, 333.
(27) Bader, R. F. W. *Atoms in Molecules: A Quantum Theory*; Clarendon Press: Oxford, U.K., 1990.
(28) Biegler-König, F. W.; Bader, R. F. W.; Tang, T. H. *J. Comput. Chem.* **1982**, *3*, 317.
(29) Popelier, P. L. A. *MORPHY98, A Topological Analysis Program*, version 0.2; University of Manchester (UMIST), Manchester, U.K., 1999.
(30) Alkorta, I.; Picazo, O. *Arkivoc* **2005**, *ix*, 305.
(31) Reed, A. E.; Curtiss, L. A.; Weinhold, F. *Chem. Rev.* **1988**, *88*, 899.
(32) Glendening, E. D. ; Badenhoop, K.; Reed, A. E.; Carpenter, J. E.; Bohmann, J. A.; Morales, C. M.; Weinhold, F. *NBO 5.0*; Theoretical Chemistry Institute, University of Wisconsin: Madison, WI, 2001.
(33) Glendening, E. D. *J. Am. Chem. Soc.* **1996**, *118*, 2473–2482.
(34) GAMESS, version 11: Schmidt, M. W.; Baldridge, K. K.; Boatz, J. A.; Elbert, S. T.; Gordon, M. S.; Jensen, J. H.; Koseki, S.; Matsunaga, N.; Nguyen, K. A.; Su, S. J.; Windus, T. L.; Dupuis, M.; Montgomery, J. A. *J. Comput. Chem.* **1993**, *14*, 1347–1363.
(35) (a) Alkorta, I; Rozas, I.; Elguero, J. *J. Org. Chem.* **1997**, *62*, 4687. (b) Mascal, M.; Armstrong, A.; Bartberger, M. *J. Am. Chem. Soc.* **2002**, *124*, 6274. (c) Alkorta, I.; Rozas, I.; Elguero, J. *J. Am. Chem. Soc.* **2002**, *124*, 8593. (d) Quiñonero, D.; Garau, C.; Rotger, C.; Frontera, A.; Ballester, P.; Costa, A.; Deyà, P. M. *Angew. Chem., Int. Ed.* **2002**, *41*, 3389. (e) Alkorta, I; Blanco, F.; Elguero, J. *J. Phys. Chem. A* **2008**, *112*, 6753.
(36) Hinds, K.; Holloway, J. H.; Legon, A. C. *Chem. Phys. Lett.* **1995**, *242*, 407.
(37) Legon, A. C.; Soper, P. D.; Keenan, M. R.; Minton, T. K.; Balle, T. J.; Flygare, W. H. *J. Chem. Phys.* **1980**, *73*, 583.
(38) Goodwin, E. J.; Legon, A. C. *Chem. Phys.* **1984**, *87*, 81.
(39) Yaron, D.; Peterson, K. I.; Zolandz, D.; Klemperer, W.; Lovas, F. J.; Suenram, R. D. *J. Chem. Phys.* **1990**, *92*, 7095.
(40) McIntosh, A. L.; Wang, Z.; Lucchese, R. R.; Bevan, J. W.; Legon, A. C. *Chem. Phys. Lett.* **1999**, *305*, 57.
(41) Wang, Z.; Lucchese, R. R.; Bevan, J. W.; Suckley, A.; Rego, C. A.; Legon, A. C. *J. Chem. Phys.* **1993**, *98*, 1761.
(42) Pimentel, G. C.; McClellan, A. L. *The Hydrogen Bond*; Freeman: San Francisco, CA, 1960.
(43) Hobza, P.; Havlas, Z. *Chem. Rev.* **2000**, *100*, 4253.
(44) Alkorta, I.; Rozas, I.; Elguero, J. *Chem. Soc. Rev.* **1998**, *27*, 163.
(45) Bone, R. G. A.; Bader, R. F. W. *J. Phys. Chem.* **1996**, *100*, 10892.
(46) Alkorta, I.; Barrios, L.; Rozas, I.; Elguero, J. *THEOCHEM* **2000**, *496*, 131.
(47) Espinosa, E.; Alkorta, I.; Elguero, J.; Molins, E *J. Chem. Phys.* **2002**, *117*, 5542.
(48) Bofill, J. M.; Olivella, S.; Solé, A.; Anglada, J. M. *J. Am. Chem. Soc.* **1999**, *121*, 1337.
(49) Alkorta, I.; Elguero, J. *J. Chem. Phys.* **2002**, *117*, 6463.
(50) Prieto, P.; de la Hoz, A.; Alkorta, I.; Rozas, I.; Elguero, J. *Chem. Phys. Lett.* **2001**, *350*, 325.
(51) Mata, I.; Alkorta, I.; Espinosa, E.; Molins, E. Elguero, J. Topological Properties of the Electron Distribution in Hydrogen Bonded Systems. In *The Quantum Theory of Atoms in Molecules*; Matta, C. F., Boyd, R. J., Eds.; Wiley-VCH: Weinheim, Germany, 2007.

JP810462H